

## The Exhumation of the Western Greater Caucasus; a Thermochronometric Study

Stephen J. Vincent, Andrew Carter, Vladimir A. Lavrishchev, Samuel P. Rice, Teimuraz G. Barabadze and Niels Hovius

## APPENDIX

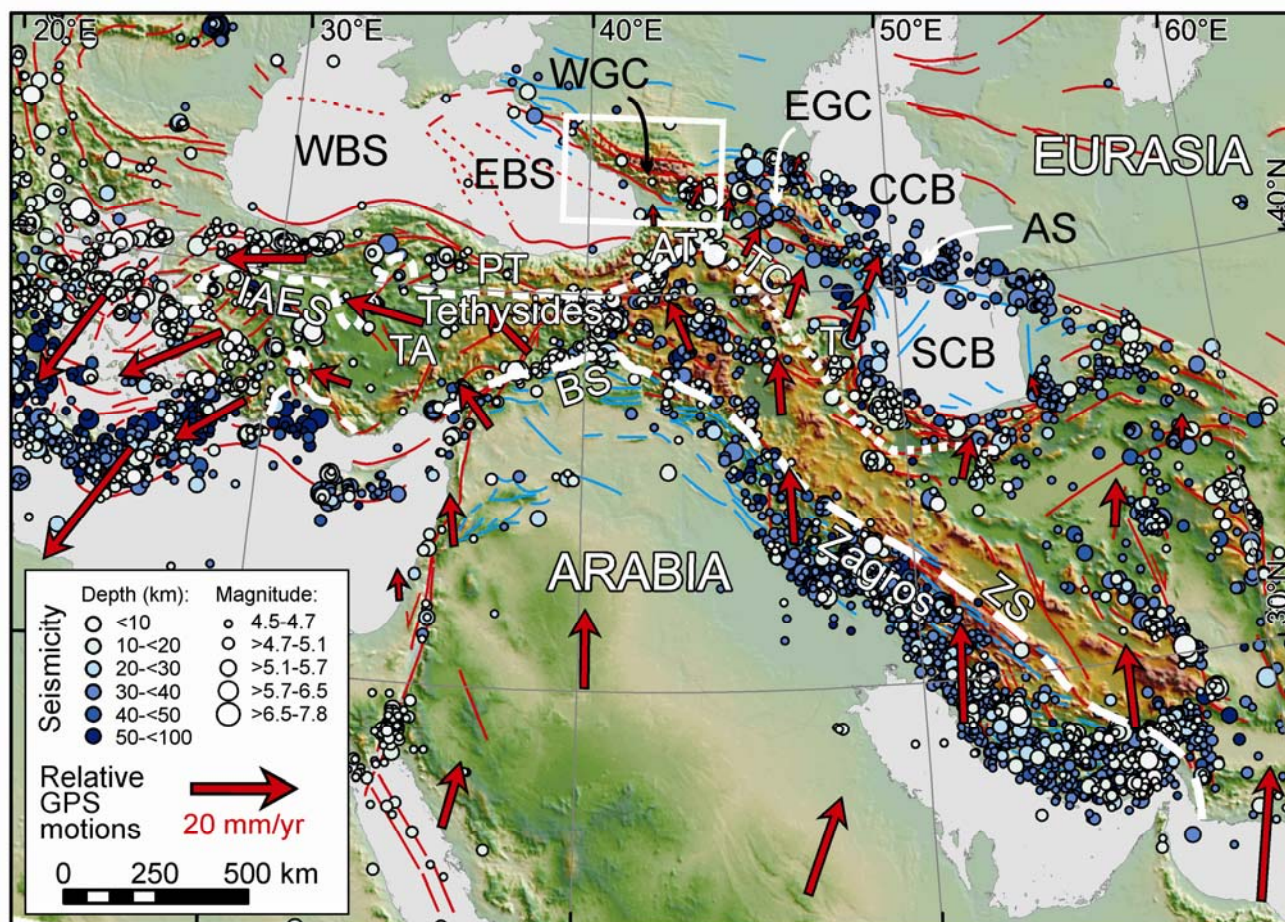


Figure 1. Schematic tectonic map showing the Greater Caucasus at the northern margin of the Arabia–Eurasia collision zone, the current GPS-constrained motion of the region relative to stable Eurasia and the occurrence of instrumentally recorded earthquakes  $M \geq 4.5$ . Structures are extended from Allen *et al.* (2003), GPS motions are taken from Reilinger *et al.* (2006) and the seismicity record from the US National Earthquake Information Center catalogue (1973–June 2009). The study area is highlighted in the box and selected Neotethyan suture zones shown by dashed lines. Abbreviations: AS – Apsheron sill; AT – Adjara–Trialet belt; BS – Bitlis suture; CCB – Central Caspian Basin; EBS – Eastern Black Sea; EGC – eastern Greater Caucasus; IAES – İsmir–Ankara–Erzincan suture; PT – Pontides; SCB – South Caspian Basin; T – Talysh; TA – Taurides–Anatolides; TC – Transcaucasus; WBS – Western Black Sea; WGC – western Greater Caucasus; ZS – Zagros suture.

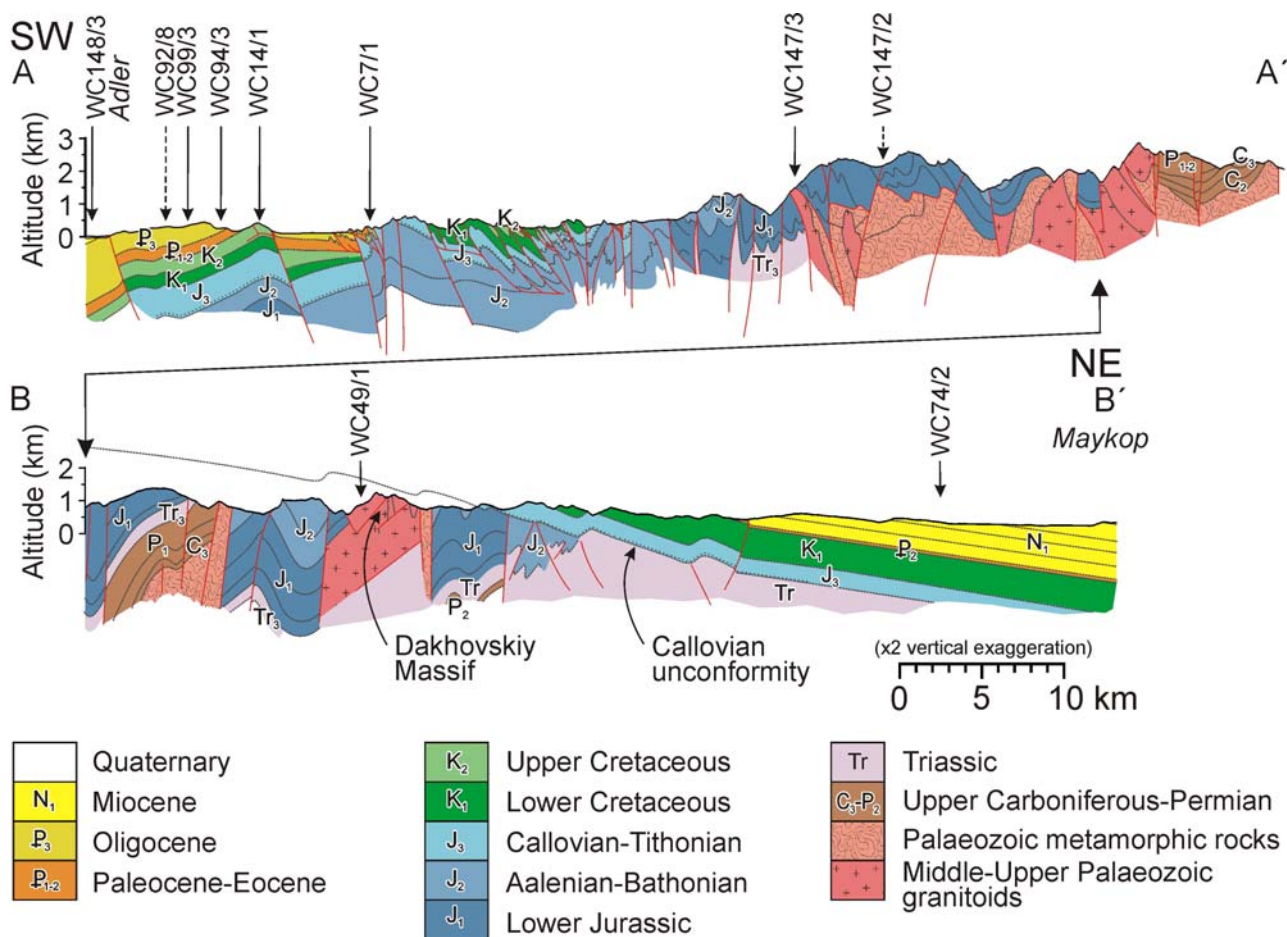


Figure 3. Cross-section through the western Greater Caucasus based on original field observations and the mapping of Melnikov, Srabony'an & Kokarev (1994) and Lavrishchev, Prutskiy & Semenov (2002). For location see Figure 2.



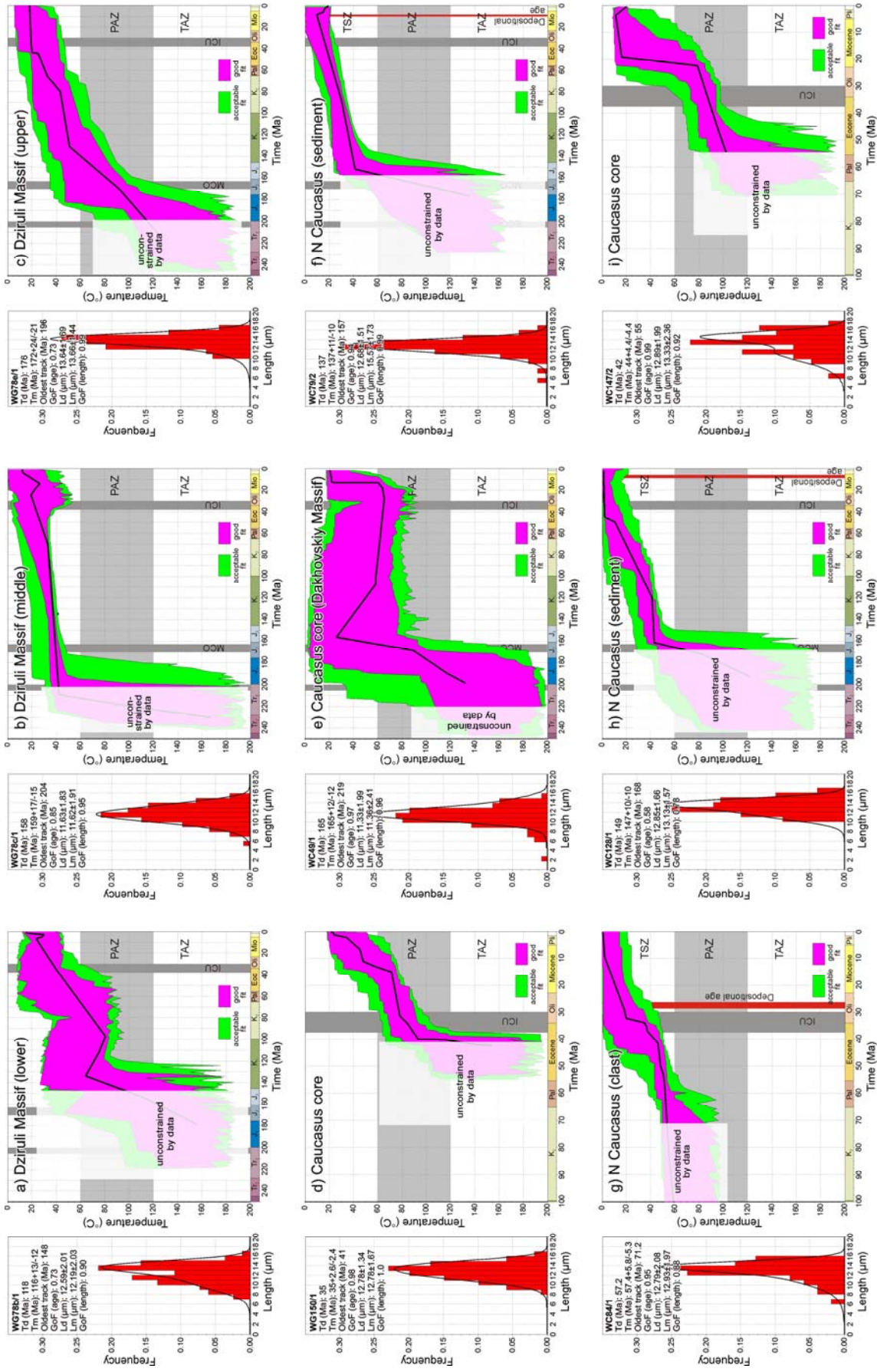
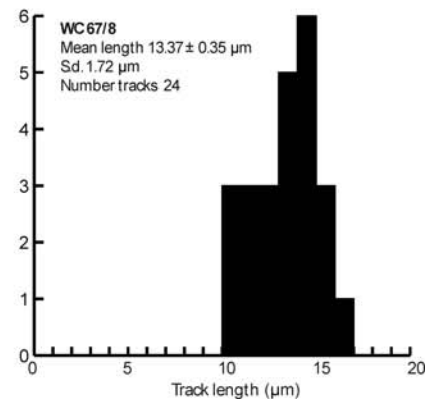
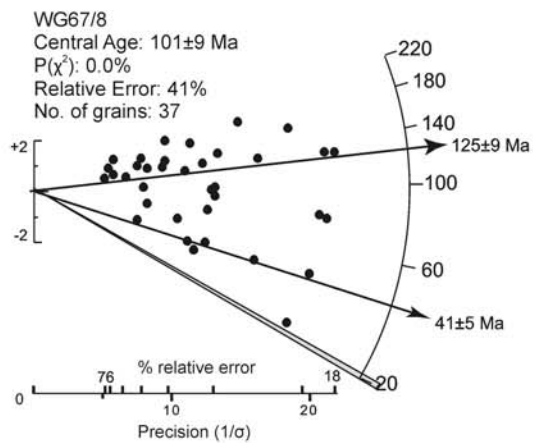
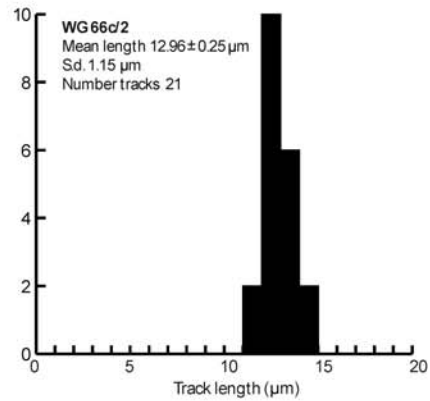
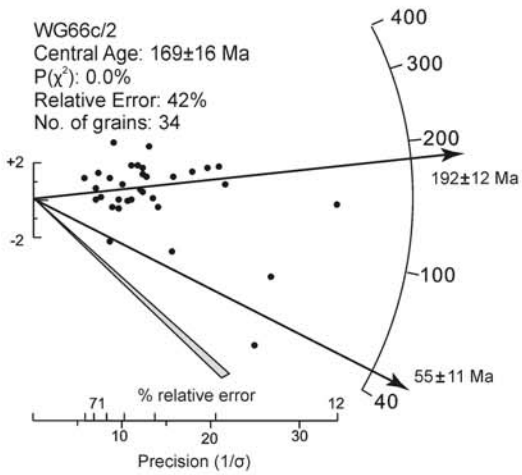
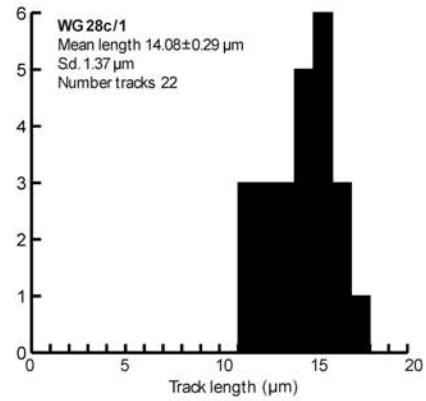
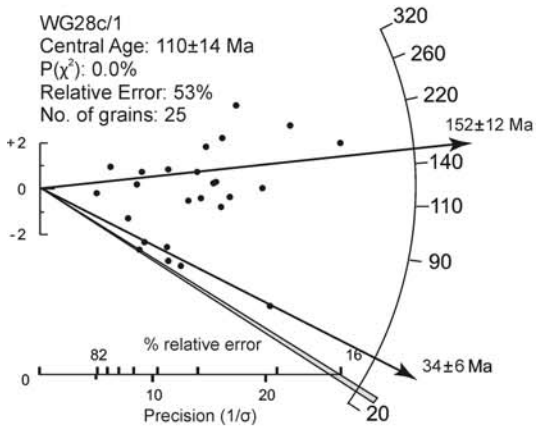
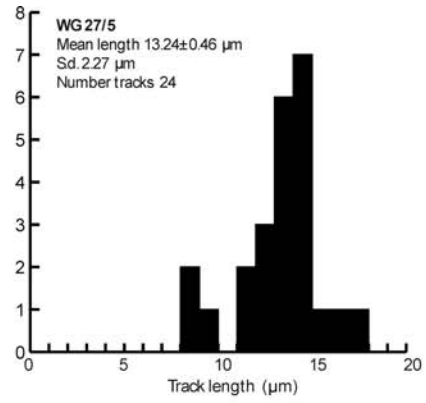
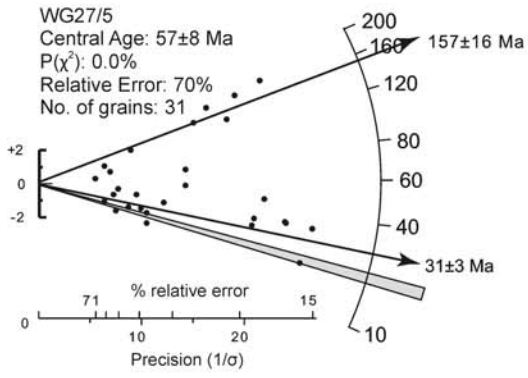
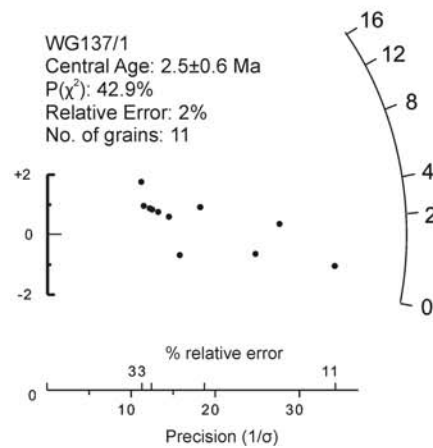
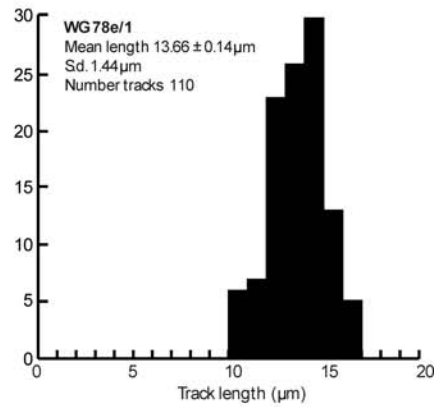
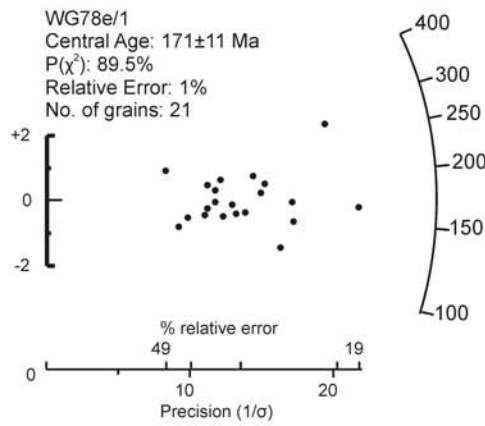
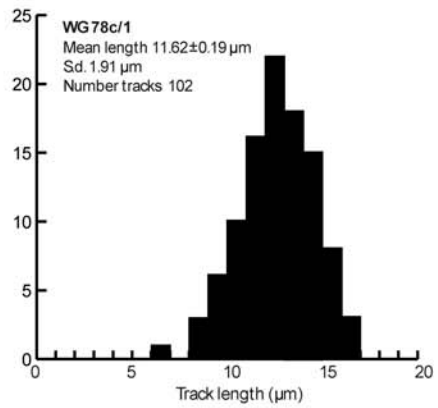
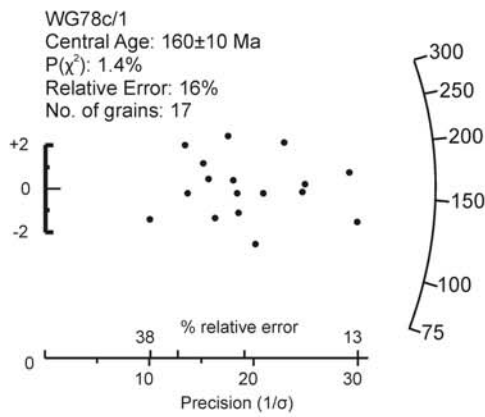
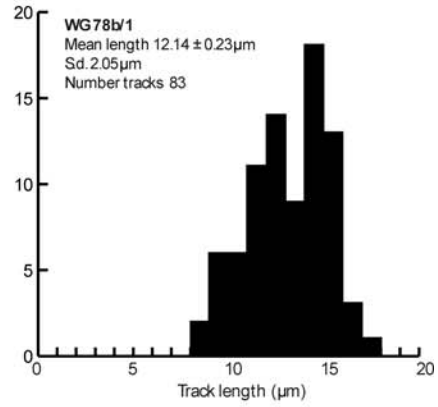
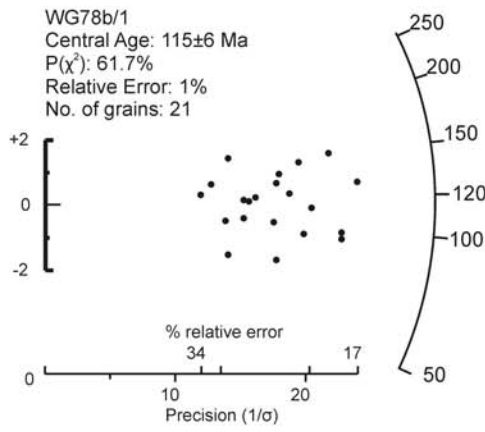


Figure 5. Best-fit thermal models for AFT samples from the Dziruli Massif and western Greater Caucasus listed in alpha-numeric order. One hundred good thermal paths were obtained for each model. The approximate intervals of the ECO (early Cimmerian orogeny), MCO (middle Cimmerian orogeny) and ICU (initial Caucasus uplift) are shown as the approximate temperature ranges of the apatite TAZ (total annealing zone), PAZ (partial annealing zone) and TSZ (total stability zone). The purple and green shaded areas encompass  $1\sigma$  (good) and  $2\sigma$  (acceptable) confidence limits, respectively, and the lines correspond to the most probable thermal histories. Goodness of fit (Gof) gives an indication of the fit between observed and predicted values (values close to 1 are best). The geological timescale is from Gradstein, Ogg and Smith (2004).

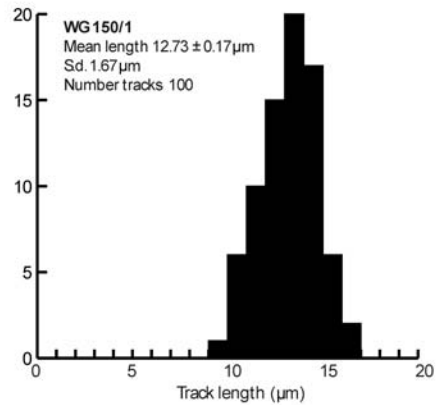
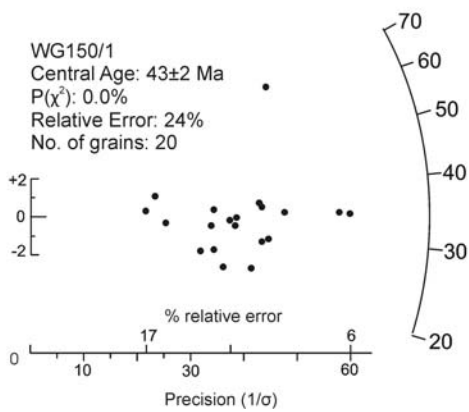
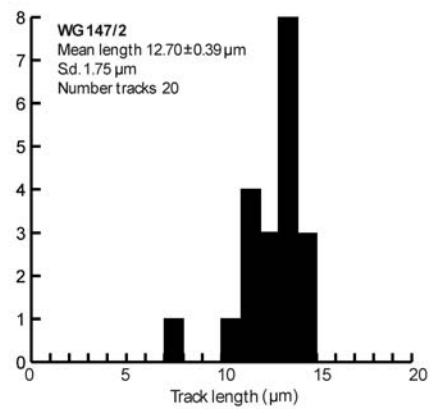
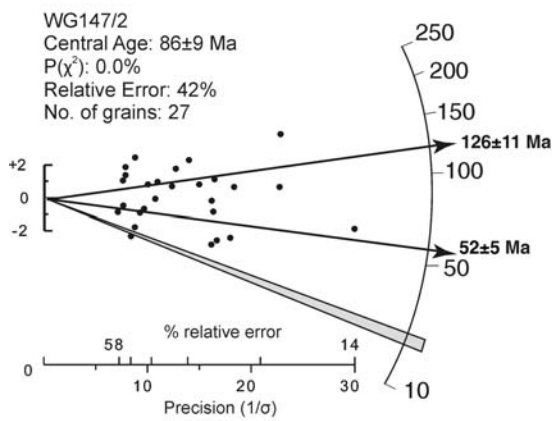
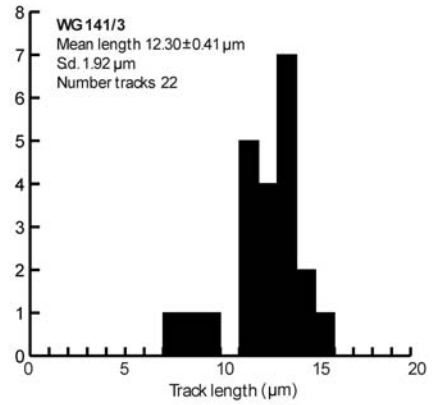
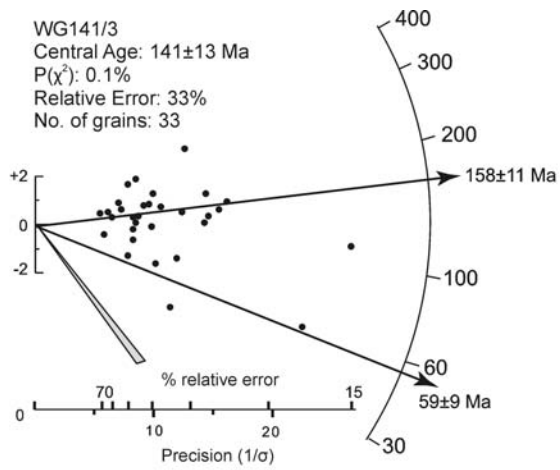
Sample	Mean track length (µm)	S.D.	No. tracks	3	4	5	6	7	8	9	10	11	12	13	14	15	16	17	Mean Cl wt%
WG27/5	13.24±0.46	2.27	24	0	0	0	0	0	2	1	0	2	3	6	7	1	1	1	
WG28c/1	14.08±0.29	1.37	22	0	0	0	0	0	0	0	0	2	2	6	5	6	1	0	0.0 - 5
WG66c/2	12.96±0.25	1.15	21	0	0	0	0	0	0	1	0	2	10	6	2	0	0	0	0-1.5
WG67/8	13.37±0.35	1.72	24	0	0	0	0	0	0	0	0	3	3	3	5	6	3	1	0.0 - 5
WG78b/1	12.14±0.23	2.05	83	0	0	0	0	0	2	6	6	11	14	9	18	13	3	1	0.75
WG78c/1	11.62±0.19	1.91	102	0	0	0	1	0	3	6	10	16	22	18	15	8	3	0	0.00
WG78e/1	13.66±0.14	1.44	110	0	0	0	0	0	0	0	0	6	7	23	26	30	13	5	0.80
WG137/1	No length data																		
WG141/3	12.30±0.41	1.93	22	0	0	0	0	1	1	1	0	5	4	7	2	1	0	0	0.0 - 5
WG147/2	12.70±0.39	1.75	20	0	0	0	0	1	0	0	1	4	3	8	3	0	0	0	0 - 1.9
WG149/1	No data																		
WG150/1	12.73±0.17	1.67	100	0	0	0	0	0	0	1	6	10	15	20	23	17	6	2	<0.05
WG151/1	No data																		
WC7/1	Too few																		
WC14/1	14.36±0.21	1.49	50	0	0	0	0	0	0	0	1	10	13	10	9	5	1	1	
WC39/2	12.39±0.35	1.63	22	0	0	0	0	0	0	2	3	2	11	21	22	21	8	7	1
WC49/1	11.36±0.20	2.00	100	1	0	0	0	2	3	3	11	21	22	21	8	7	1	0	0-0.4
WC74/2	No data																		
WC79/2	12.57±0.20	2.03	74	0	0	1	0	1	0	2	5	12	22	17	10	3	1	0	
WC84/1	12.93±0.20	1.97	101	0	0	0	0	2	0	4	4	6	8	23	25	16	13	0	0-0.4
WC92/8	12.79±0.51	1.62	10	0	0	0	0	0	0	0	1	3	2	2	1	1	0	0	
WC94/3	No data																		
WC99/3	13.18±0.28	1.29	20	0	0	0	0	0	0	0	1	4	3	6	5	1	0	0	
WC120/1	13.43±0.47	1.71	13	0	0	0	0	0	0	0	1	3	1	2	4	1	1	0	
WC123/1	13.75±0.43	1.54	13	0	0	0	0	0	0	0	0	0	0	5	4	1	1	2	
WC128/1	13.12±0.16	1.57	100	0	0	0	0	0	0	0	1	10	13	10	9	5	1	1	
WC133/2	No data																		
WC147/2	13.33±0.37	2.36	40	0	0	0	0	1	0	0	2	3	6	3	9	6	4	6	
WC147/3	14.14±0.21	2.05	100	0	0	0	0	2	1	2	2	5	15	14	15	22	4	5	
WC148/3	None																		
WC149/3	12.99±0.38	1.78	21	0	0	0	0	0	1	0	0	0	0	5	5	3	6	1	

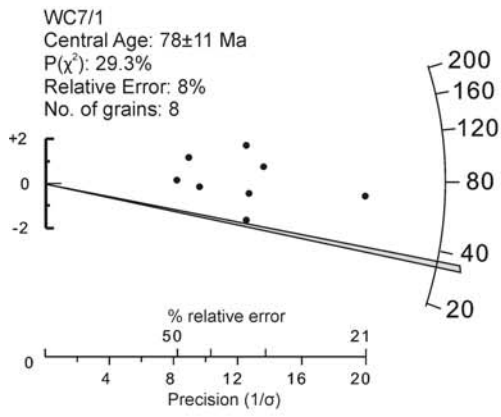
Table A1. Apatite track length data and sample mean composition



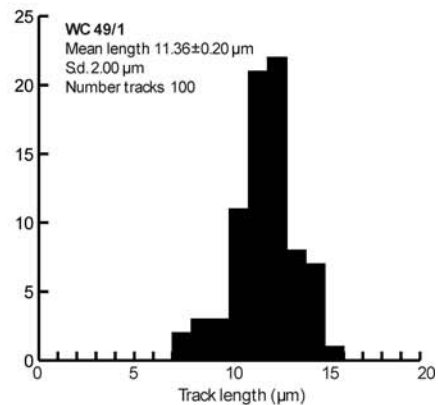
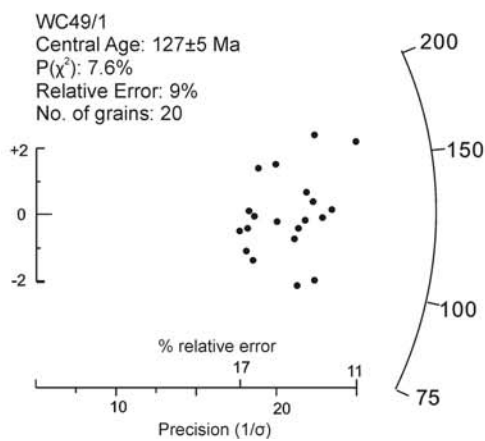
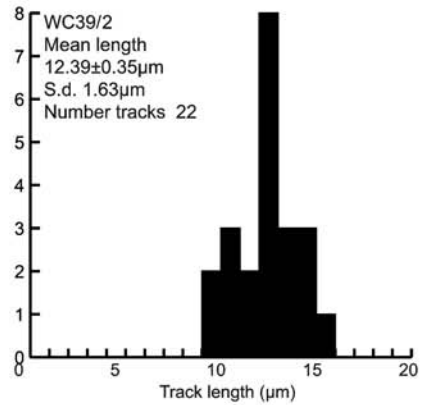
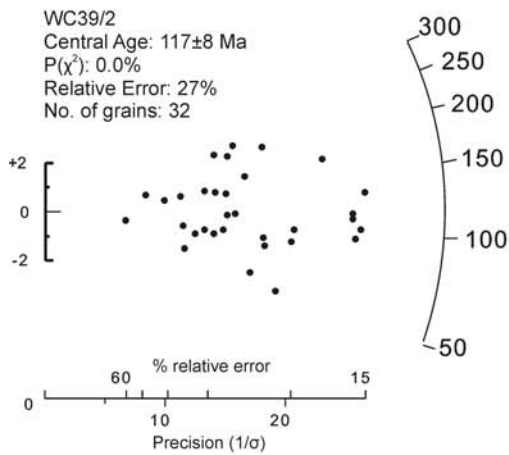
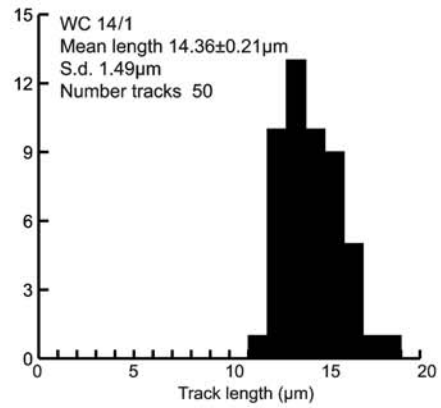
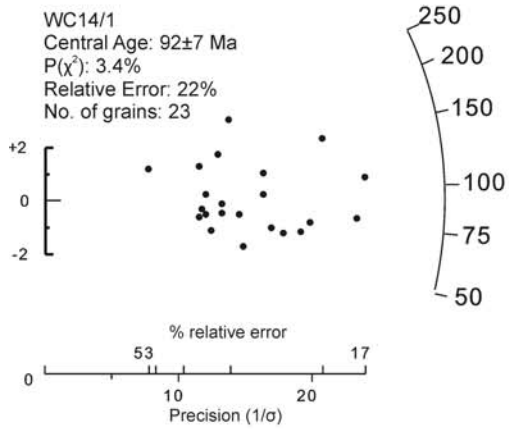


no track length data

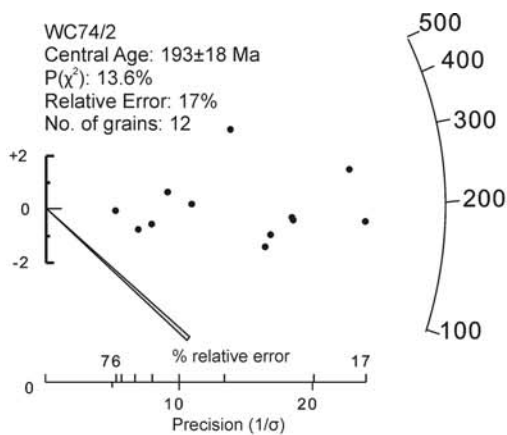




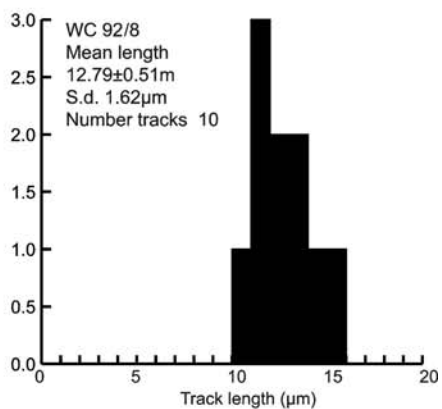
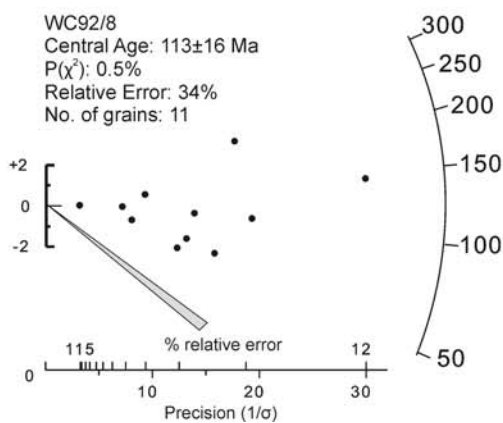
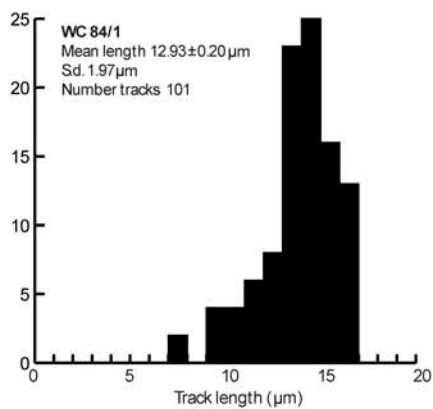
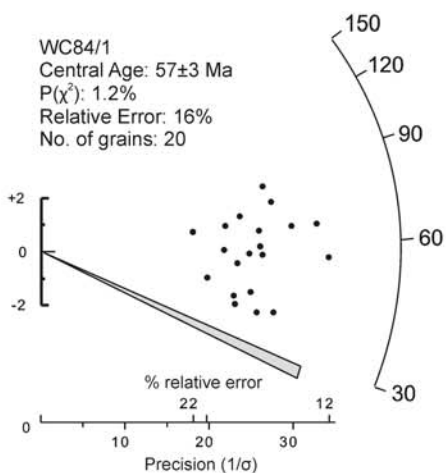
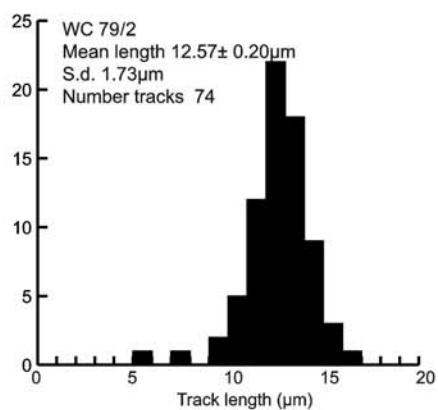
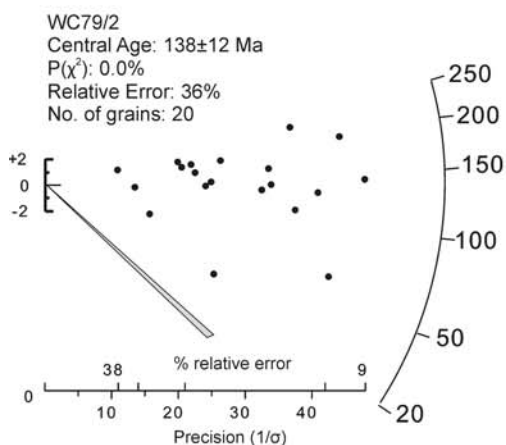
no track length data

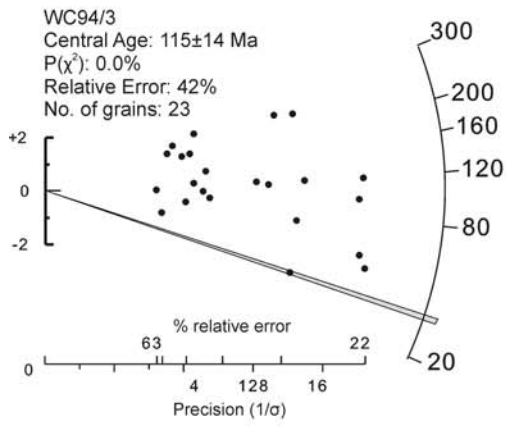




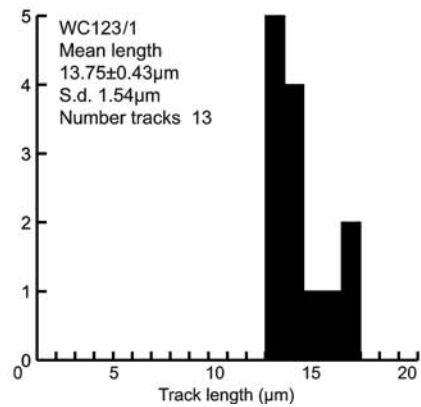
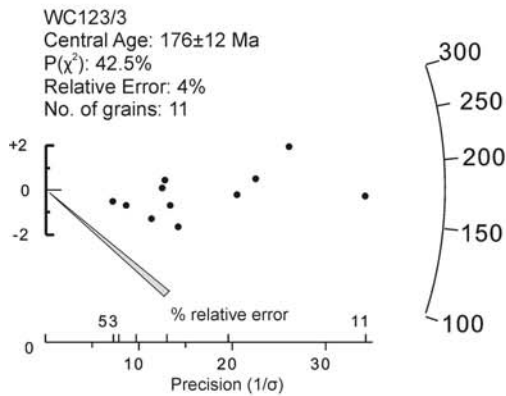
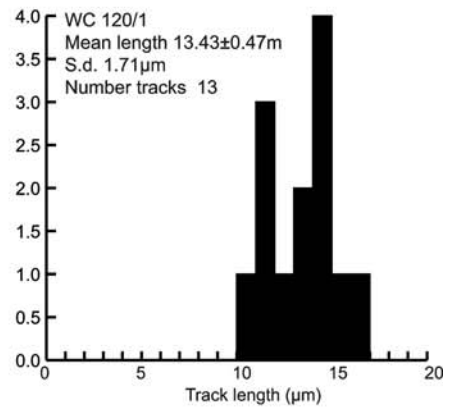
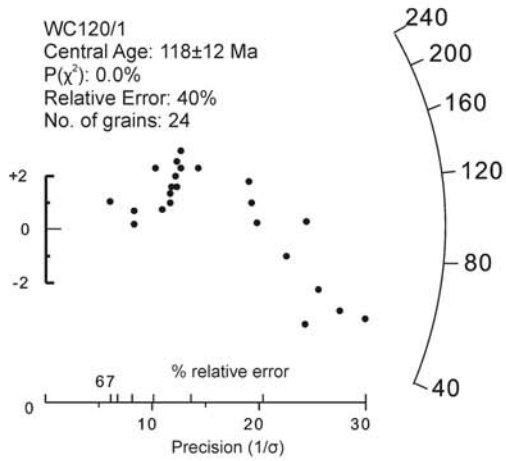
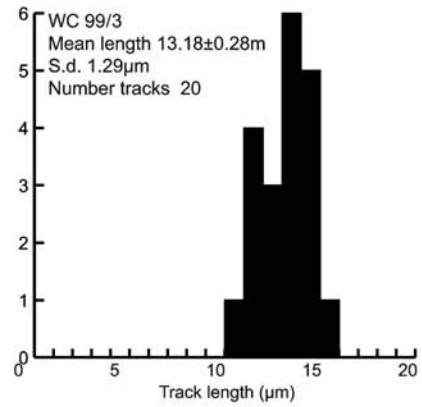
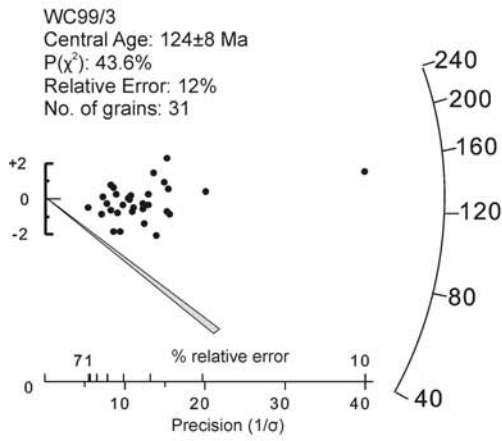


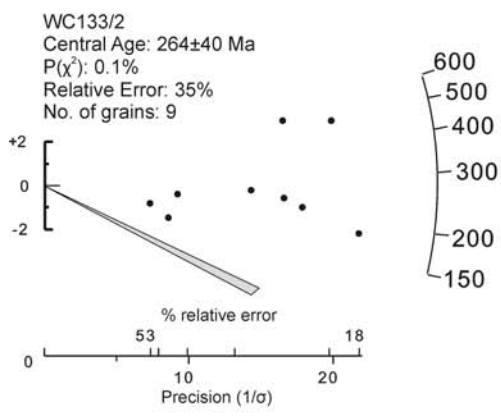
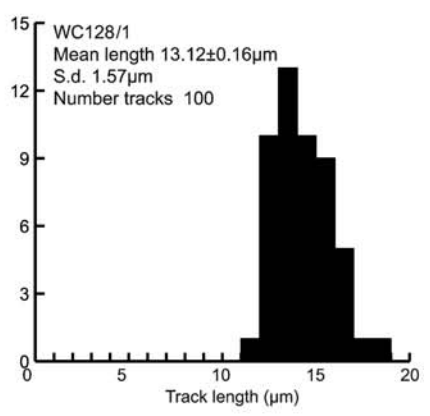
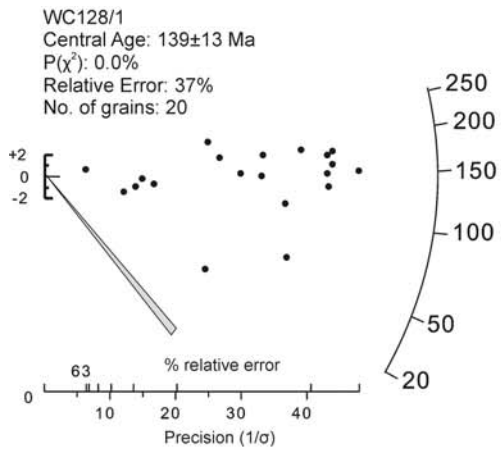
no track length data



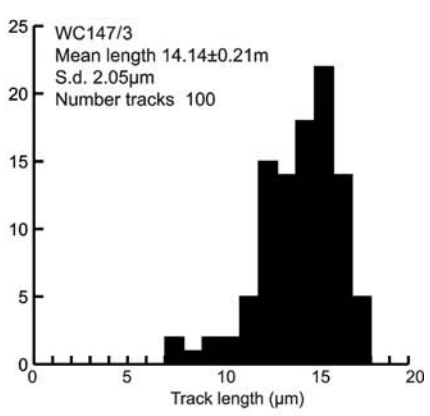
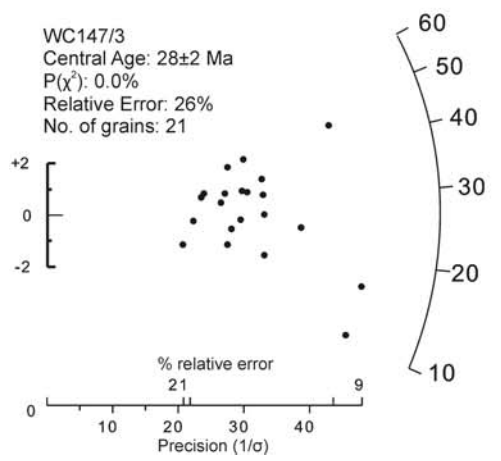
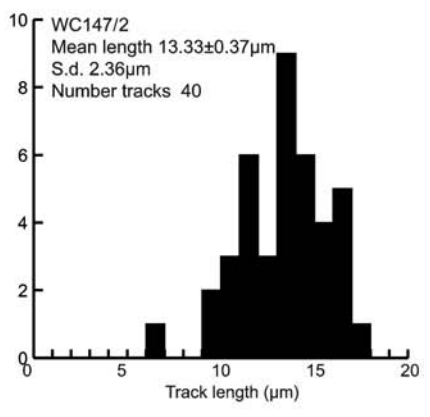
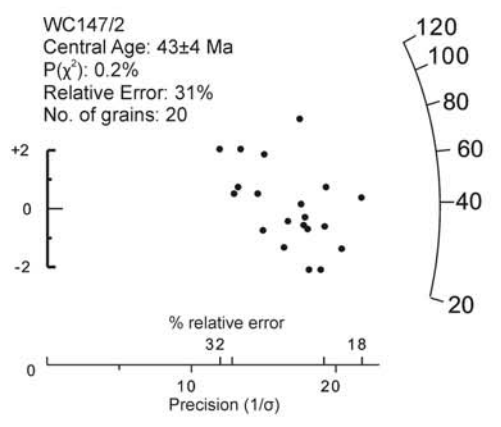


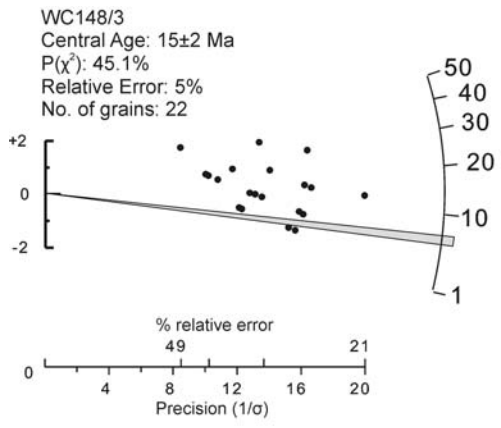
no track length data





no track length data





no track length data

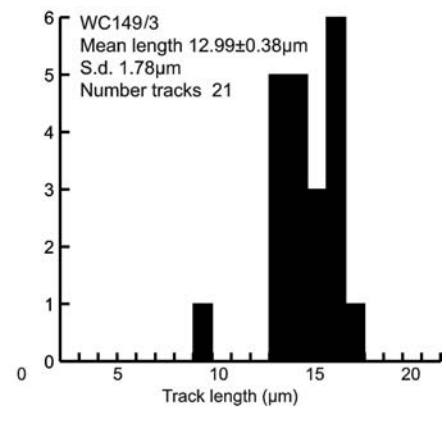
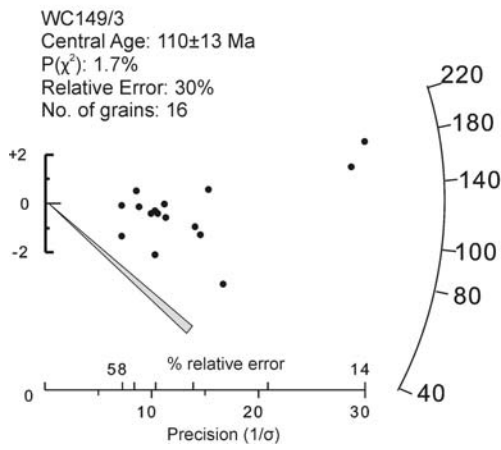


Figure A1. Radial plots of apatite track length distributions